Published in final edited form as:
J Alzheimers Dis. 2012 ; 32(1): 217–232. doi:10.3233/JAD-2012-120478.

Broad-Based Nutritional Supplementation in 3x Tg Mice Corrects Mitochondrial Function and Indicates Sex-Specificity in Response to Alzheimer's Disease Intervention

Andrew B. Wolf[a,b,i], **B. Blair Braden**[b,i], **Heather Bimonte-Nelson**[b,i], **Yael Kusne**[a,b,i], **Nicole Young**[a,b,i], **Elizabeth Engler-Chiurazzi**[b,i], **Alexandra N. Garcia**[b,i], **Douglas G. Walker**[c,i], **Guna S.D. Moses**[c,d,i], **Hung Tran**[c,i], **Frank LaFerla**[e], **LihFen Lue**[c,i], **Nancy Emerson Lombardo**[f,g], and **Jon Valla**[a,h,i,*]

[a]Barrow Neurological Institute, St. Joseph's Hospital and Medical Center, Phoenix, AZ, USA

[b]Arizona State University, Tempe, AZ, USA

[c]Banner Sun Health Research Institute, Sun City, AZ, USA

[d]Grand Canyon University, Phoenix, AZ, USA

[e]Institute for Memory Impairments and Neurological Disorders, University of California, Irvine, CA, USA

[f]Department of Neurology, Boston University School of Medicine, Boston, MA, USA

[g]Veterans Administration Medical Center, Bedford, MA, USA

[h]Midwestern University, Glendale, AZ, USA

[i]Arizona Alzheimer's Consortium, Phoenix, AZ, USA

Abstract

Nutrition has been highlighted as a potential factor in Alzheimer's disease (AD) risk and decline and has been investigated as a therapeutic target. Broad-based combination diet therapies have the potential to simultaneously effect numerous protective and corrective processes, both directly (e.g., neuroprotection) and indirectly (e.g., improved vascular health). Here we administered either normal mouse chow with a broad-based nutritional supplement or mouse chow alone to aged male and female 3×Tg mice and wildtype (WT) controls. After approximately 4 months of feeding, mice were given a battery of cognitive tasks and then injected with a radiolabeled glucose analog. Brains were assessed for differences in regional glucose uptake and mitochondrial cytochrome oxidase activity, AD pathology, and inflammatory markers. Supplementation induced behavioral changes in the 3×Tg, but not WT, mice, and the mode of these changes was influenced by sex. Subsequent analyses indicated that differential response to supplementation by male and female 3×Tg mice highlighted brain regional strategies for the preservation of function. Several regions involved have been shown to mediate responses to steroid hormones, indicating a mechanism for sex-based vulnerability. Thus, these findings may have broad implications for the human response to future therapeutics.

*Correspondence to: Jon Valla, Department of Biochemistry, Midwestern University, 19555 N. 59th Avenue, Glendale, AZ 85308, USA. Tel.: +1 623 572 3729; Fax: +1 623 572 3679; jvalla@midwestern.edu.

Authors' disclosures available online (http://www.j-alz.com/disclosures/view.php?id=1379).

Keywords

Biomarkers; cytochrome-c oxidase (Complex IV); diet therapy; memory; sex; transgenic mice

INTRODUCTION

Alzheimer's disease (AD) is a neurodegenerative condition that is the most prevalent cause of dementia in the elderly. Due to shifting demographics, it is projected that the number of AD cases worldwide will increase dramatically during the first half of the 21st century [1]. While study of early-onset AD has uncovered genetic mutations that modulate production of the amyloid-β (Aβ) protein thought to be key in the disease, the vast majority (>98%) of AD cases are late-onset and idiopathic. Because of the limited knowledge of the underlying cellular and molecular causes of late-onset AD, detailed examination of risk factors is essential for developing a stronger understanding of the pathogenic process. Based on the existence of dozens of epidemiological studies demonstrating that nutrition is an important factor in susceptibility to AD [2], several ongoing or recently completed human trials have investigated the neuroprotective capacities of many different nutrients [3]. In addition to these human trials, the wide-availability of AD rodent models has allowed for multiple experimental studies, with a significant body of work supporting the role of nutrients in modulating disease-related cognitive decline and pathology: blueberry supplementation can avert both cognitive decline and deficits in signal transduction [4], curcumin demonstrates an ability to prevent cognitive decline [5], green tea can slow cognitive decline through multiple mechanisms [6, 7], and both cinnamon extracts [8] and grape polyphenol extracts [9] can inhibit Aβ oligomerization and cognitive decline. Additionally, omega-3 fatty acids can reduce Aβ burden [10–13], improve cognition [14], and protect from dendritic pathology [10,15]. Medical food "cocktails" can reverse cognitive decline and attenuate soluble Aβ pathology [16], and the nutritional supplement S-adenosyl methionine has recently been shown to be effective in delaying tau or Aβ pathology in 3×Tg mice [17] and may have wide-ranging effects on amyloid levels, tau phosphorylation, and DNA methylation [18].

Whereas, until recently, most studies of dietary intervention in animal models largely have been focused on examining the effects of a single nutrient, the Memory Preservation Nutrition Supplement Program (MPNSP) used here combines three separate broad-based supplements: a phyto-nutrient powder, high-quality fish oil, and an amalgam of herbs and spices based on an evidence-based integrated whole foods program, Memory Preservation Nutrition [19]. The MPNSP was designed to delay the onset and slow the progression of AD in humans by providing broad-based nutritional supplementation targeting multiple organs and pathways. In this study, we administered this supplementation regimen to the 3×Tg mouse, which is the first transgenic mouse harboring the $PS1_{M146v}$, $A\beta PP_{Swe}$, and tau_{P301L} transgenes, and therefore recapitulates several hallmarks of AD, including concomitant plaque and tangle formation in AD-vulnerable regions [20]. We hypothesized that this dietary cocktail could extend and enhance the established successes shown in single nutrient studies due to additive and synergistic effects across the multiple nutrients. As a further benefit, these products have been demonstrated to be well-tolerated [21, 22] and are considerably less expensive than most conventional pharmaceutical treatments. We hypothesized that the MPNSP would prevent or reverse the brain regional glucose uptake declines we have shown in a variety of murine models of AD [23–26].

Human fluorodeoxyglucose positron emission tomography (FDG PET) studies show that region-specific alterations in the cerebral metabolic rate for glucose (CMRgl) are found in AD, with hypometabolism present in the posterior cingulate-precuneus (PCC), parieto-temporal, and prefrontal regions [27, 28]. Interestingly, decrements in CMRgl are localized

to these same regions in aged presymptomatic homozygotes [27] and young-adult carriers [29] of the APOEε4 allele, the primary genetic risk factor for late-onset AD. We extended these findings to demonstrate reduced mitochondrial function, as measured by cytochrome c oxidase activity (Complex IV of the electron transport chain), in postmortem PCC as well as isolated platelets from living AD patients [30, 31]. Further, the same deficiency was measured in platelets from patients with mild cognitive impairment (MCI) [30], and in the PCC of young-adult (18–40 year-old) carriers of the APOE ε4 allele in the absence of AD histopathology [32], the latter thus indicating that, along with the CMRgl changes, energy metabolism decline may be among the earliest detectable brain changes associated with AD risk. This indicates that mitochondrial functional decline, measured via cytochrome oxidase (Complex IV), is effective at detecting some of the earliest cellular-level changes in AD pathogenesis or vulnerability and is therefore an attractive biomarker for use in evaluation of interventions and therapeutics, particularly those aimed at preclinical and early-stage AD. Thus, in addition to behavioral cognition and brain regional FDG uptake, we analyzed mitochondrial cytochrome oxidase activity, as well as fibrillar and soluble AD pathology and neuroinflammatory markers.

MATERIALS AND METHODS

This study was performed under protocols approved by the respective Institutional Animal Care and Use Committees at the Barrow Neurological Institute, St. Joseph's Hospital and Medical Center and Arizona State University (ASU). 3×Tg and wildtype (WT) controls (129/sv × C57BL6) were bred in our colony at the Barrow Neurological Institute from founders received from the University of California, Irvine. Transgene and diet status were blinded until analyses were complete. 3×Tg (n = 28, 14/condition) and WT (n= 28, 14/condition) mice were placed in age-and sex-matched 4-mouse cohorts, with one mouse of each genotype fed supplementation and the other standard diet (below). Mice were group housed in Plexiglas shoebox-style cages prior to study start and housed in singly or in pairs once supplementation began, with access to food (supplemented or standard) and water *ad libitum*.

Supplementation

Dietary supplementation was initiated at an average age of 38 weeks (range 29–46 weeks) and continued for 25 weeks, until the mice were euthanized. Mice on the supplemented condition were fed LabDiet 5001 (Purina, St. Louis, MO) containing the supplemental phyto-nutrient powder, herbal/spice amalgam, and cod liver oil integrated into the chow (for respective compositions, see Table 1). Dose calculations were based on the MPNSP-recommended dose to an 80 kg human scaled to a 35 g mouse consuming 4 g/day. Mice on the nonsupplemented condition were fed LabDiet 9F 5020 (Purina, St. Louis, MO). Daily food consumption was monitored for the first three weeks, and mice were weighed every third week for the duration of the study. After approximately 18 weeks, all mice were transferred from the Barrow Neurological Institute to ASU to undergo behavioral testing; they remained at ASU until euthanized. Figure 1 provides a flowchart of the experimental protocols.

Delayed match to position three choice task

Mice were tested on the Delayed Match to Position (DMP) Three Choice Task for 6 trials/day for 10 days, evaluating spatial working and short-term memory retention. A black Plexiglas maze (each arm was 38.1 cm × 12.7 cm) with four open arms, was filled with water made opaque using non-toxic paint, average temperature 17.5°C, and contained one escape platform. The platform was moved to a new arm each day, but remained in the same arm within a day. Trial one was the information trial informing the animal where the

platform was for that day's session, trial two was the working memory test trial, and trials three through six were recent memory test trials [33]. Mice were given 90 s to find the platform. Once located, the animal remained on the platform for 15 s. The inter-trial interval (ITI) was 30 s. An arm entry was counted when the tip of a mouse's snout reached a mark 11 cm into the arm. First errors were first entries into an arm without a platform, and Repeat errors were repeat entries into an arm without a platform. The dependent variables were the number of Total errors (First + Repeat errors), First errors, and Repeat errors across testing (i.e., days 1–10, trials 2–6) for each treatment group. To investigate the effects of learning versus asymptotic phases of testing, errors were blocked into days 1–5 versus days 6–10. For all measures of regular testing, an omnibus ANOVA was run to investigate main effects and interactions. When significant, analyses were followed by *post hoc t*-tests.

On day 11, mice were given a delay challenge of a 30 min ITI between trials 5 and 6. Planned comparisons to analyze effects of the delay were run comparing errors on the baseline day/trial of day 10, trial 6 (the last day of regular testing) versus the post delay trial given on day 11, trial 6. Effects of $p \leq 0.05$ were considered significant.

Morris water maze (MWM)

Two days after DMP concluded, each mouse received 4 trials/day for 6 days using a tub (188 cm diameter) filled with opaque water using non-toxic paint (average temperature 17.5°C). The hidden platform (10 cm wide) remained in a fixed location, thereby testing spatial reference memory [34, 35]. Mice were placed in the maze from the North, South, East, or West location, and had 60 s to locate the platform in the Northeast quadrant. Once the mouse found the platform, the trial was terminated and the mouse remained there for 15 s. The mouse was then placed into its heated cage until its next trial with an approximate ITI of 10 min. Performance was assessed by swim path distance (cm) and latency (s) to the platform. To evaluate whether mice localized the platform to the spatial location, after all test trials on day 6, a 60 s probe trial was given with the platform removed. Percent of total distance in the previously platformed (target) quadrant was compared to the quadrant diagonally opposite the platform. For each trial, a camera suspended above the maze tracked each mouse's path and a tracking system (Ethovision 5.1, Noldus Instruments) analyzed each mouse's tracing. Distance and latency across all days of testing and percent distance in the target and opposite quadrants during the probe trial were analyzed via an omnibus ANOVA to investigate main effects and interactions. When significant, analyses were followed by *post hoc t*-tests. Effects of $p \leq 0.05$ were considered significant.

Tissue processing

Each animal was given an i.p. injection of 18 μCi/100 g body weight [^{14}C]-FDG (American Radiolabeled Chemicals, St. Louis, MO) in sterile saline. During the subsequent 45 min uptake period each animal was placed into an empty individual cage in a dark and quiet cabinet. Mice were then decapitated, and the brain rapidly extracted and frozen. Brains were stored at −20°C until sectioned. 40 μm coronal sections were taken in four series, creating three matched slide sets and an aliquot of tissue divided into 3 pools (anterior to hippocampal formation, containing hippocampal formation, and posterior to hippocampal formation) for each subject. At each level of the series, 4 sections were also cut at 20 μm and dried for later immunohistochemistry. FDG autoradiography and cytochrome oxidase (CO) histochemistry and subsequent densitometric imaging proceeded as performed previously [25, 36].

Image analysis

Defined regions-of-interest (ROIs) corresponded to those presented in Paxinos & Franklin [37], with the exception that the retrosplenial gyrus was divided into three defined

anteroposterior ROIs to localize any reductions in PCC, based on previous work [25]: posterior cingulate (approximately bregma −1.4), posterior cingulate level 2 (bregma −2.1), and retrosplenial (bregma −2.6). Autoradiographic and histochemical data were analyzed independently; based on the behavioral outcomes, sex was included as a variable in omnibus 2×2×2 (genotype by supplementation by sex) analyses of variance, with $\alpha = 0.05$. Significant effects were followed by *post hoc* Student's *t*-tests at $\alpha = 0.05$: we did not correct for multiple comparisons but report the calculated *p* values; while this does not minimize Type I errors, the results are consistent with our previous analyses. Individual ROI scores showing a Studentized residual >3.0 in the ANOVA were deemed to be outliers and removed from the final analysis.

Fibrillar amyloid and tau pathology

For Thioflavin S staining for amyloid plaques, slides were fixed with 4% buffered paraformaldehyde (PFA), rinsed with tap water, rinsed in distilled H_2O, immersed in 4% thioflavin S in distilled H_2O for 5 min, differentiated in 70% ethanol, rinsed twice with distilled H_2O, and coverslipped with aqueous mounting media. Immunohistochemistry for hyper-phosphorylated tau (clone AT8) was performed on frozen coronal sections. Frozen sections were fixed with 4% PFA, blocked with hydrogen peroxide (3% for 5 min) and 3% bovine serum albumin and 2% goat serum (1 h), and probed on-slide with an antibody for phosphorylated tau (AT8; Pierce) and visualized with diaminobenzidine-hydrochloride (Dako LSAB+ System). Assessments of both were performed by a single rater, blinded to conditions, on an Olympus BX61 microscope using a 3-point scale (heavy, moderate, light) in the areas of highest deposition/tangle density (hippocampal subiculum, CA1, CA3).

Brain tissue extract for ELISA and western blotting

Ten of the cryostat-cut coronal sections, from each of the 3 levels, were homogenized in 200 μl of 50 mM Tris-HCl at pH 8.0, with 1 mM EDTA and a cocktail of protease and phosphatase inhibitors (Pierce); these were aliquoted and stored until the ELISA. For Aβ ELISA, samples were further extracted with guanidine HCl, whereas for glial fibrillar acidic protein (GFAP) and synaptophysin ELISA, samples were further extracted in 4 volumes of 5x RIPA buffer.

Aβ ELISA

Thirty μl of Tris buffer-extracted brain homogenates were extracted further with 7M guanidine-HCl to obtain a final concentration of 5M guanidine-HCl. Extraction was performed at 4°C for 17 h on shaker. Protein concentrations of these samples were determined by MicroBCA assay. ELISA kits for human $A\beta_{42}$ and $A\beta_{40}$ (Invitrogen) were used according to manufacturer's instructions. For both $A\beta_{42}$ and $A\beta_{40}$ ELISA, 1200 ng of protein were loaded to each well, and duplicate wells from the same samples were assayed and averaged.

GFAP ELISA

The GFAP ELISA was developed in-house, using a capture antibody of purified anti-GFAP cocktail (BD Biosciences) used at 0.25 μg in 100 μl per well, and a detection antibody of rabbit polyclonal anti-GFAP (DAKO) used at 1:10,000 dilution. Anti-rabbit IgG-conjugated horseradish peroxidase (rabbit IgG-HRP; Pierce) was used at 1:20,000 dilution. Purified GFAP (Calbiochem) was used to manufacture standards to cover a range from 0.156 to 10 ng/ml. Capture antibody coating buffer was sterile PBS, pH 7.4. Wash buffer was composed of PBS with 0.05% Tween 20 (PBST), pH 7.4. Sample dilution buffer was PBST with 1% skim milk while blocking buffer contained 3% skim milk powder. Plates were coated with capture antibody for 18 h at 4°C, followed by washing 5 times with wash buffer installed in

a plate washer. Plates were blocked for 1 h using blocking buffer at room temperature, followed by washing 5 times. RIPA buffer-extracted brain samples were loaded at 100 μg per 100 μl per well for 2h, and detection antibody incubation was carried out for 2h after washing 5 times. Anti-rabbit IgG-HRP diluted in wash buffer was applied to the wells for 2 h followed by 5x wash. Colorimetric enzymatic reaction was achieved by incubating 30 min with substrate for anti-rabbit HRP (R&D Systems). Reaction was stopped by 1M sulfuric acid solution. Optical absorbance for the color products in each well was read by a spectrophotometer at 450 nm. Data was calculated according to the linear regression of the protein standards and absorbance.

Synaptophysin ELISA

Synaptophysin ELISA was also developed in-house, using a capture antibody of mouse anti-synaptophysin IgM antibody (Covance, clone SP17) used at 1:4000; detection antibody was rabbit anti-synaptophysin IgG (Chemicon) used at 1:2000. Synaptophysin protein standard (Abnova) was used in a range from 0.156 to 5 ng/ml. Samples were loaded to each well at 1 μg protein per 100 μl per well. Anti-rabbit IgG-HRP (Pierce) was used at 1: 3000. Wash buffer was 0.1M Tris buffer, pH 7.4, containing 0.05% Tween 20 (TBT). Sodium carbonate buffer, pH 9.6, was used as coating buffer for the capture antibody. Blocking buffer was TBT containing 5% skim milk, while sample diluent was TBT containing 2% skim milk powder. Incubation schedule was performed as described above.

Western blot detection of microglial markers

Protein (10 μg/lane) from brain samples prepared for ELISA was prepared for electrophoresis with LDS loading buffer and reducing reagent DTT (1 μg/μl) and run on NuPage 10–14% Bis-Tris mini gels with MES running buffer (Invitrogen). Separated proteins were transferred to nitrocellulose membranes at 30 volts for 60 min. Membranes were air-dried and blocked with 50 mM Tris-buffered saline, pH 8.0, containing 0.05% Tween 20 (TBS-T) and 5% nonfat dried milk powder. Microglial specific marker Iba-1 (ionized calcium binding adapter protein 1) was detected with a rabbit polyclonal antibody (Wako Chemicals USA, Richmond, VA). Microglial alternative activation markers Ym1 (chitinase 3-like 3), MMR1 (macrophage man-nose receptor 1), and ARG1 (arginase 1) were detected with polyclonal antibodies raised in either goat or sheep (R&D Systems, Minnesota), followed by secondary antibodies conjugated with HRP of appropriate species. Blots were then reacted with Dura chemiluminescent substrate for HRP (Thermo Scientific) and imaged. Specific bands were identified by appropriate molecular weight and the density of immunoreactive bands was measured with Alpha View software (Cell Biosciences) and normalized to β-actin.

RESULTS

MPNSP supplementation was generally well-tolerated. Mortality during the study appeared unrelated to supplementation: 1 WT mouse and 3 3×Tg mice died or were euthanized prematurely due to illness while on supplementation, and 2 WT and 4 3×Tg mice died or were euthanized while on the standard diet. Data from these animals are included when possible and when not obviously impacted by illness preceding death. Final sample sizes under supplementation were n=12 3×Tg (6M, 6F) and n=10WT (4M, 6F), and nonsupplemented were n=13 3×Tg (5M,8F) and n=13WT (5M, 8F). Consumption of the two diets did not differ during the initial 3-week monitoring period; overall, each supplemented mouse consumed 3.8 ± 0.5 g/day and each mouse on standard chow 3.8 ±0.6 g/day (p = 0.89,2-tailed t-test; Fig. 2A). Mean body weight in the two groups diverged early in the feeding (3–6 weeks) and then stabilized, with supplemented mice weighing less in comparison at each point (Fig. 2B), but there was no indication of increasing divergence

between the groups over time. Given the relatively broad range in age of mice at initiation of supplementation, we first explored the possibility of age-related effects by analyzing behavioral, FDG, and CO data by similarly-aged cohorts (approximately 29–35 weeks, 36–41 weeks, and 42–46 weeks at initiation), and via ANCOVA with age as covariate; no significant effects of age were found (data not shown). In contrast, analysis of the behavioral results demonstrated that sex accounted for more measured variability than age; thus, all subsequent analyses included sex as a variable.

Delayed match to position three choice task

Across all days of regular testing, there was a main effect of genotype for each type of error [Total: $F(1, 45) = 6.103$, $p < 0.05$ (Fig. 2A); First: $F(1, 45) = 8.359$, $p < 0.01$; Repeat: $F(1, 45) = 4.694$ $p < 0.05$] with 3×Tg mice making more errors than WT mice. To investigate the effects of learning versus asymptotic phases of testing, errors were blocked by days 1–5 versus days 6–10. Here there was a significant interaction between block, genotype, and sex [$F(1, 41) = 7.390$, $p < 0.01$]. During the asymptotic phase, the supplemented male 3×Tg mice made fewer total errors than the nonsupplemented male 3×Tg mice [$t(8) = 5.267$, $p = 0.05$ (Fig. 3)]. The female 3×Tg mice did not differ by supplement status.

On day 11 there was a 30 min delay given between trials 5 and 6. No group significantly increased the number of errors committed between trial 6 of the last day of regular testing (day 10) and trial 6 after the delay (day 11).

Morris water maze

Across all days of testing, there was a main effect of day for distance and latency in the WT and 3×Tg mice [WT Distance: $F(5, 130) = 117.887$; $p < 0.0001$; WT Latency: $F(5, 130) = 104.124$; $p < 0.0001$; 3×Tg Distance: $F(5, 90) = 21.396$; $p < 0.0001$; 3×Tg Latency: $F(5, 90) = 15.428$; $p < 0.0001$], with scores decreasing across days, demonstrating learning of the task for both genotypes. There was a main effect of genotype for each measure [Distance: $F(1, 44) = 9.671$, $p < 0.005$; Latency: $F(1, 44) = 7.995$, $p < 0.01$] with 3×Tg mice swimming a longer distance and exhibiting a greater latency to locate the platform, than WT mice (Fig. 4). There were no supplementation effects, sex effects, day × supplementation interactions, nor day × sex interactions for performance as measured by either measure. The probe trial, assessing learning of the platform location (NE quadrant), revealed a main effect of quadrant [$F(1, 36) = 240.994$; $p < 0.0001$] and a quadrant × genotype interaction [$F(1, 36) = 9.799$; $p < 0.005$]. Each group spent more percent distance in the target NE quadrant as compared to the opposite SW quadrant, showing localization of the platform location [WT: $F(1, 22) = 392.851$; $p < 0.0001$; 3×Tg: $F(1, 18) = 40.375$; $p < 0.0001$]; however, WT mice spent significantly more percent distance in the target NE quadrant [$t(40) = 14.747$; $p < 0.0005$] and significantly less percent distance in the opposite quadrant SW [$t(36) = 4.747$; $p < 0.05$] than 3×Tg mice.

FDG autoradiography

The omnibus 2×2×2 ANOVA revealed a significant main effect ($p < 0.05$) of genotype in 44 of 55 ROIs, consistent with our previous results in these mice at a slightly older age (18 months; [25]). Also consistent with previous results, our usual data normalization to average whole brain activity was precluded by the widespread gene-related changes in glucose uptake, so analysis proceeded with nonnormalized FDG uptake data. Modestly significant main effects of supplement status were found (reticular thalamus, nucleus basalis, and medial geniculate), and within these, significant interactions between genotype and supplementation (medial geniculate) and genotype, supplementation, and sex (nucleus basalis). Completion of *post hoc* 2-tailed *t*-tests revealed that significant effects in medial geniculate were mediated by a supplement-driven increase in WT mice (supplemented

versus nonsupplemented:871± 210 versus 657 ± 122, mean ± standard deviation, $p = 0.009$), particularly the males (supplemented versus nonsupplemented: 921 ± 176 versus 605 ± 40, $p = 0.025$). A similar trend was apparent in male WT nucleus basalis (supplemented versus nonsupplemented: 826 ± 167 versus 498 ± 68, $p = 0.020$). Four other ROIs showed the identical relationship: middle cingulate gyrus ($p = 0.012$), anteroventral thalamus ($p = 0.020$), reticular thalamus ($p = 0.033$), and mediodorsal thalamus ($p= 0.041$). Only one ROI showed a similar effect in WT females, the mammillary bodies (1226 ± 148 versus 869 ± 249, $p= 0.011$). Of note, significant effects of the supplementation were seen across the expanse of the WT cingulate gyrus: anterior ($p = 0.047$), middle ($p = 0.039$), posterior ($p = 0.039$), retrosplenial ($p = 0.034$), except posterior level 2 ($p = 0.094$), and also in the heavily interconnected hippocampal subiculum ($p = 0.042$). WT somatosensory barrel fields, lateral posterior thalamus, and pontine nuclei also showed significant effects of supplementation ($p < 0.05$). All significant changes were increases, and collectively, all WT ROI values were increased in the supplemented group. No significant *post hoc* effects were seen across the 3×Tg groups or between comparisons of sex within the 3×Tg; all apparent regional glucose uptake effects were mediated by changes in WT mice.

Cytochrome oxidase histochemistry

Previous analyses of 3×Tg mice from our colony have demonstrated significant CO activity declines in several brain regions (unpublished data), similar to our findings in other AD mouse models [36]. The omnibus 2×2×2 ANOVA revealed many regional significant main effects (Table 2). Several strong interactions with sex were identified, prominently including the entorhinal cortex and hippocampal formation subregions. Significant differences between subgroups of 3×Tg mice were again confirmed by *post hoc* 2-tailed *t*-tests. In contrast to FDG uptake, the CO changes under supplementation were mediated almost exclusively by 3×Tg mice: supplementation induced significant increases in several brain regions, to approximately WT levels (Fig. 5A), most significantly in posterior cingulate (3×Tg supplemented versus nonsupplemented: $p < 0.001$), primary somatosensory ($p = 0.001$) and barrel field ($p = 0.009$) cortex, mediodorsal thalamus ($p = 0.003$), lateral hypothalamus ($p = 0.007$), and lateral posterior thalamus ($p= 0.013$). A similar trend was apparent in basolateral amygdala. The directionality and effect size of these changes was roughly the same in 3×Tg males and females. However, an alternate pattern emerged when comparing across sex in areas showing other significant ANOVA effects (Fig. 5B): in entorhinal cortex, male and female 3×Tg showed a significant difference after supplementation (201 ± 16 and 166 ± 20, $p= 0.039$), but 3×Tg males *increased* significantly to WT levels, while 3×Tg females *decreased* nonsignificantly from WT levels, indicating a profound difference in regional function. Such a trend was also apparent in CA1 and the medial mammillary nuclei. Similarly, in CA3 and dentate gyrus, supplementation elicited little change in 3×Tg males but caused the females to significantly *decline* from WT levels (Fig. 5B).

Fibrillar amyloid and tau pathology

Thioflavin staining for amyloid deposition revealed a consistent involvement of the hippocampal formation, particularly the anterodorsal subiculum and CA1, but often extending through ventroposterior aspects and to the amygdala. Lesser deposition was also seen in the basal forebrain and frontal cortices. This pattern is consistent with our previous report [25]. All WT mice were negative, and no apparent differences were observed between supplementation conditions in the 3×Tg mice. AT8-positive structures resembling neurofibrillary tangles were consistently located in 3×Tg hippocampal CA1 and CA3; in images captured from these areas, no apparent difference in the density or composition of these tangles was seen between supplementation conditions. In the case of both Aβ and tau, deposition tended to worsen with increasing age across the range studied here.

Biochemical measurements of Aβ, synaptophysin, and glial activation markers

ELISA measurement of $A\beta_{40}$ and $A\beta_{42}$ in 3×Tg mouse brain tissues at the level containing hippocampus showed a trend toward lower levels in supplemented mice. Analyzing by gender, it was apparent that the trend was driven by female mice, which showed significantly higher levels compared to the males. Further analysis of the 3×Tg female subgroup (age at sacrifice [weeks]: supplemented: 64.1 ±2.5; nonsupplemented: 67.0 ±2.0, n = 5/group) showed a significant reduction in $A\beta_{42}$ (Fig. 6A; $p < 0.038$). This phenomenon was not observed in $A\beta_{40}$ or male mice, although the trend in $A\beta_{40}$ was similar in 3×Tg females. The concentration of synaptophysin was not affected by supplementation (Fig. 6B).

Activated astroglial marker, GFAP, was used as an initial indicator of neuroinflammation. Supplementation did not lead to differential GFAP levels in either WT or 3×Tg mice (Fig. 6C). To determine the effects of diet treatment on microglial activation, we measured whether there were changes in the levels of Iba1, Ym1, MMR1, and ARG1 expressions. Iba1 has been used widely as a marker for brain microglia across a spectrum of activation states, whereas Ym1, MMR1, and ARG1 have been used specifically to identify alternatively-activated microglia in AD and AβPP transgenic mouse brains [38]. Western blotting results showed a lack of effect of supplementation on most of the microglial markers except on ARG1 in female 3×Tg mice ($p < 0.05$, Fig. 7).

DISCUSSION

We have confirmed that MPNSP supplementation can modulate markers of brain energy metabolism and alter other indicators of cognition and pathophysiology in a mouse model of AD. MPNSP supplementation prevented or reversed cognitive decline, with the modality affected dependent upon sex in this model. In *post hoc* analyses, MPNSP supplementation increased WT FDG uptake in several regions, including retrosplenial cingulate, posterior cingulate, and subiculum, but showed few effects in the 3×Tg mice, who maintained significant FDG decreases in most ROIs. In contrast, analysis of regional CO activity in the 3×Tg demonstrated several key regions in which the enzyme activity was corrected to WT levels. Following on the behavioral analysis, a breakdown by sex revealed striking differences in brain regional effects, particularly in regions in and closely connected to the hippocampal formation (e.g., entorhinal cortex).

Deposition of fibrillar plaques and AT8-positive tau did not appear to be ameliorated by the supplementation, possibly a function of the timing of intervention: evidence of intracellular and extracellular Aβ in the 3×Tg mice has been reported at 4 and 6 months, respectively [39]. Memory impairment has been reported at 4 months [39] and synaptic dysfunction at 6 months [20]. Our earliest intervention began at approximately 7 months, after these processes should be underway; that said, biochemical measurements of the levels of human $A\beta_{40}$ and $A\beta_{42}$ in 3×Tg mice showed supplementation-induced changes, with a strong trend toward differences dependent upon sex. A significant $A\beta_{42}$-lowering effect was observed in the female subgroup, which had much higher Aβ levels overall as reported in this model previously [40]. Our analyses indicate that our sample may have been underpowered for detection of several of the tested effects; alternatively, an earlier start time or higher dosing may be required to maximize the benefit of broad-based nutritional supplementation.

Our earlier regional FDG analyses of mouse models of AD, including this model [25], indicated consistent declines in brain regional FDG uptake, some similar to those seen in human AD [27, 28]. We were surprised to find that the supplementation did not correct this aberrant FDG uptake, which is an extremely plastic marker of brain activity, while it did correct mitochondrial CO function, also a plastic marker but much less so, in many of the same regions. One possible explanation for this dichotomy may be that aspects of the

transgene-induced changes have direct and perhaps irreversible effects on mechanisms of FDG uptake, while the mitochondrial changes may be more amenable to our treatment, which includes compounds thought to be mitochondrial enhancers [41].

Concerning cognition, we were able to detect robust differences between the WT and 3×Tg groups for both spatial working and short-term memory on the DMP task, and spatial reference memory on the MWM, establishing an excellent paradigm for the evaluation of interventions in the 3×Tg AD model. Importantly, MPNSP supplementation generated significant changes in short-term spatial memory as demonstrated in the DMP task, but not for spatial reference memory on the MWM. These divergent effects may represent a specificity of memory type enhancement through MPNSP supplementation, aiding more in short-term working memory functional recovery rather than reference memory. Indeed, these effects are in line with the brain region-specific recovery of CO activity in supplemented male 3×Tg entorhinal cortex, an area that may be more important for short-term working memory processing than long-term reference memory, as shown in patients with MCI using MRI voxel-based morphometry [42]. Although behavioral analysis often revealed only marginal effects of the supplementation, we could determine that subject sex contributed substantially to variability and, when analyzed accordingly, differences between the sexes were indeed significant. Further, in the subsequent imaging and pathology analyses, including sex as a covariate illuminated other sex-specific changes. Specifically, in entorhinal cortex, medial mammillary nuclei, and in the CA3 and dentate gyrus of the hippocampus, a pattern emerged whereby in these regions supplementation corrected CO activity to WT levels in 3×Tg males only, and decreased levels in supplemented 3×Tg females only. Given the prominent role of these nuclei in the behavioral tasks tested, these regional effects may reflect the sex-specific performance differences we observed. It follows then, that these network differences may reflect differences between male and female correction and/or compensation of functional deficits; i.e., 3×Tg females activate different pathways than males in order to perform the task, or suffer enhanced regional vulnerability (or differences in recovery) which forces them to do so. That the entorhinal cortex and hippocampus appeared central to this sex-specific network change in mitochondrial activity was no surprise; previous research from our group has indicated that these regions are particularly sensitive to sex steroid-induced alterations in female rodents [43]. In fact, estrogen and progesterone have been shown to modulate AD pathology and hippocampal-dependent behavioral function in 3×Tg mice [44], and female 3×Tg mice display larger deficits in hippocampal-dependent behavior than matched males [45]. The CO biomarker identified changes in areas (including the hippocampal formation) relevant to the apparent preservation of cognitive function that resulted from supplementation in 3×Tg males. This lends support to further examination of CO as an endpoint in preclinical interventional studies, and our concomitant work in humans [30–32] indicates that CO may be a useful biomarker early in the disease process and a quantifiable endpoint for the effects of consequential intervention.

As many components of the supplement diet used in this study may possess anti-inflammatory properties, we also examined whether the diet could alter the activation of glial cells. We found that in female 3×Tg mice the supplementation significantly increased the expression levels of ARG1, a marker for alternative activation of microglia. This result suggested that the supplementation might have potential to shift a subpopulation of microglia from classical to alternative activation phenotype. Alternatively-activated microglia have an enhanced ability to phagocytize Aβ [38]. However, ARG1 expression could also be increased with severity of AD as indicated by previous data obtained in AD brains and in 70 week-old Tg2576 mice, an animal model for amyloid pathology in AD [36]. Increases in ARG1 have also been observed in the lipopolysaccharide-induced inflammatory response in the rTG2510 transgenic mice, an animal model over-expressing P301 L tau [46].

This study has demonstrated that broad-based nutritional supplementation can positively impact certain parameters of cognition, mitochondrial function, and pathophysiology in a transgenic mouse model of AD. There were no indications that the supplementation carried unwanted side effects; indeed, these supplements have a long history of safe use in humans, including in formal clinical trials [3, 21]. Further research is needed to establish the optimal time for such supplementation to begin and its optimal dose (in both mice and humans). The youngest mice in this study at initiation were approximately 7 months old, and cognitive deficits, Aβ accumulation, and bioenergetic deficits have been previously reported in this model prior to that age; nonetheless, MPNSP supplementation induced several potentially beneficial effects. And, while not directly addressed in this study, it is possible that supplementation may be more effective as a preventative therapy, possibly via mechanisms bolstering brain reserve (i.e., increasing metabolic capacity via effects on mitochondrial function) or keeping levels of pathological species of tau or Aβ below critical thresholds. Given the relative safety and low cost of such intervention relative to current traditional pharmaceutical treatments with similar efficacy, broad-based supplementation such as the MPNSP or comprehensive diet plans of similar design hold great promise in the prevention and potential treatment of AD.

Acknowledgments

This work supported by the Arizona Alzheimer's Consortium, an Arizona Alzheimer's Disease Core Center (P30 AG19610) Pilot Grant (JV), the Barrow Neurological Foundation (JV), the HHMI-funded ASU SOLUR Program, the Boston University Alzheimer's Disease Core Center (P30 AG013846; NEL), and the Edith Nourse Rogers Veteran's Memorial Hospital, Bedford, MA (NEL).

REFERENCES

1. Ferri CP, Prince M, Brayne C, Brodaty H, Fratiglioni L, Ganguli M, Hall K, Hasegawa K, Hendrie H, Huang Y, Jorm A, Mathers C, Menezes PR, Rimmer E, Scazufca M. Alzheimer's Disease International. Global prevalence of dementia: A Delphi consensus study. Lancet. 2005; 366:2112–2117. [PubMed: 16360788]
2. Morris MC. The role of nutrition in Alzheimer's disease: Epidemiological evidence. Eur J Neurol. 2009; 16:1–7. [PubMed: 19703213]
3. Kamphuis PJGH, Scheltens P. Can nutrients prevent or delay onset of Alzheimer's disease? J Alzheimers Dis. 2010; 20:765–775. [PubMed: 20182021]
4. Joseph JA, Denisova NA, Arendash G, Gordon M, Diamond D, Shukitt-Hale B, Morgan D. Blueberry supplementation enhances signaling and prevent behavioral deficits in an Alzheimer's disease model. Nutr Neurosci. 2003; 6:153–162. [PubMed: 12793519]
5. Yang F, Lim GP, Begum AN, Ubeda OJ, Simmons MR, Ambegaokar SS, Chen P, Kayed R, Glabe CG, Frautschy SA, Cole GM. Curcumin inhibits formation of amyloid-β oligomers and fibrils, binds plaques, and reduces amyloid *in vivo* . J Biol Chem. 2005; 280:5892–5901. [PubMed: 15590663]
6. Lee JW, Lee YK, Ban JO, Ha TY, Yun YP, Han SB, Oh KW, Hong JT. Green tea (−)-epigallocatechin-3-gallate inhibits beta-amyloid-induced cognitive dysfunction through modification of secretase activity via inhibition of ERK and NF-kappaB pathways in mice. J Nutr. 2009; 139:1987–1993. [PubMed: 19656855]
7. Rezai-Zadeh K, Shytle D, Sun N, Mori T, Hou H, Jeanniton D, Ehrhart J, Townsend K, Zeng J, Morgan D, Hardy J, Town T, Tan J. Green tea epigallocatechin-3-gallate (EGCG) modulates amyloid precursor protein cleavage and reduces cerebral amyloidosis in Alzheimer transgenic mice. J Neurosci. 2005; 25:8807–8814. [PubMed: 16177050]
8. Frydman-Marom A, Levin A, Farfara D, Benromano T, Scherzer-Attali R, Peled S, Vassar R, Segal D, Gazit E, Frenkel D, Ovadia M. Orally administrated cinnamon extract reduces β-amyloid oligomerization and corrects cognitive impairment in Alzheimer's disease animal models. PLoS One. 2011; 6:e16564. [PubMed: 21305046]

9. Wang J, Ho L, Zhao W, Ono K, Rosenweig C, Chen L, Humala N, Teplow DB, Pasinetti GM. Grape-derived polyphenolics prevent Aβ oligomerization and attenuate cognitive deterioration in a mouse model of Alzheimer's disease. J Neurosci. 2008; 28:6388–6992. [PubMed: 18562609]
10. Green KN, Martinez-Coria H, Khashwji H, Hall EB, Yurko-Mauro KA, Ellis L, LaFerla FM. Dietary docosahexaenoic acid and docosapentaenoic acid ameliorate amyloid- β and tau pathology via a mechanism involving Presenilin 1 levels. J Neurosci. 2007; 27:4385–4395. [PubMed: 17442823]
11. Grimm MOW, Kuchnbecker J, Grosgen S, Burg VK, Huns dorfer B, Rothhaar TL, Friess P, de Wilde MC, Broersen LM, Penke B, Peter M, Vigh L, Grimm HS, Hartmann T. Docosahexaenoic acid reduces amyloid-β production via multiple pleiotropic mechanisms. J Biol Chem. 2011; 286:14028–14039. [PubMed: 21324907]
12. Lim GP, Calon F, Morihara T, Yang F, Teter B, Ubeda O, Salem N Jr, Frautschy SA, Cole GM. A diet enriched with the omega-3 fatty acid docosahexaenoic aicd reduces amyloid burden in an aged Alzheimer mouse model. J Neurosci. 2005; 25:3032–3040. [PubMed: 15788759]
13. Oksman M, Iivonen H, Hogyes E, Amtul Z, Penke B, Leenders I, Broersen L, Lutjohann D, Hartmann T, Tanila H. Impact of different saturated fatty acid, polyunsaturated fatty acid and cholesterol containing diets on beta-amyloid accumulation in APP/PS1 transgenic mice. Neurobiol Dis. 2006; 23:563–572. [PubMed: 16765602]
14. Arsenault D, Julien C, Tremblay C, Calon F. DHA improves cognition and prevents dysfunction of entorhinal cortex neurons in 3×Tg-AD mice. PLoS One. 2011; 6:e17397. [PubMed: 21383850]
15. Calon F, Lim GP, Yang F, Morihara T, Teter B, Ubeda O, Rostaing P, Triller A, Salem N Jr, Ashe KH, Frautschy SA, Cole GM. Docosahexaenoic acid protects from dendritic pathology in an Alzheimer's disease mouse model. Neuron. 2004; 43:633–645. [PubMed: 15339646]
16. Parachikova A, Green KN, Hendrix C, LaFerla FM. Formulation of a medical food cocktail for Alzheimer's disease: Beneficial effects on cognition and neuropathology in a mouse model of the disease. PLoS One. 2010; 5:e14015. [PubMed: 21103342]
17. Lee S, Lemere CA, Frost JL, Shea TB. Dietary supplementation with S-adenosyl methionine delayed amyloid- β and tau pathology in 3×Tg-AD mice. J Alzheimers Dis. 2011; 28:1–9.
18. Fuso A, Scarpa S. One-carbon metabolism and Alzheimer's disease: Is it all a methylation matter? Neurobiol Aging. 2011; 32:1192–1195. [PubMed: 21524430]
19. Emerson, Lombardo NB.; Volicer, L.; Martin, A.; Wu, B.; Zhang, XW. Memory preservation diet to reduce risk and slow progression of Alzheimer's disease. In: Vellas, B.; Grundman, M.; Feldman, H.; Fitten, LJ.; Winblad, B., editors. Research and Practice in Alzheimer's Disease and Cognitive Decline. New York: Springer; 2005. p. 138-159.
20. Oddo S, Caccamo A, Shepherd JD, Murphy MP, Golde TE, Kayed R, Metherate R, Mattson MP, Akbari Y, LaFerla FM. Triple-transgenic model of Alzheimer's disease with plaques and tangles: Intracellular amyloid-β. Neuron. 2003; 39:409–421. [PubMed: 12895417]
21. Capodice JL, Gorroochurn P, Cammack AS, Goluboff E, McKiernan JM, Benson MC, Stone BA, Katz AE. Zyflamend in men with high-grade prostatic intraepithelial neoplasia: Results of a phase I clinical trial. J Soc Integr Oncol. 2009; 7:43–51. [PubMed: 19476738]
22. Freund-Levi Y, Eriksdotter-Jonhagen M, Cederholm T, Basun H, Faxen-Irving G, Garlind A, Vedin I, Vessby B, Wahlund LO, Palmblad J. Omega-3 fatty acid treatment in 174 patients with mild to moderate Alzheimer disease: OmegAD study: Arandomized double-blind trial. Arch Neurol. 2006; 63:1402–1408. [PubMed: 17030655]
23. Reiman EM, Uecker A, Gonzalez-Lima F, Minear D, Chen K, Callaway NL, Berndt JD, Games D. Tracking Alzheimer's disease in transgenic mice using fluorodeoxyglu cose autoradiography. Neuroreport. 2000; 11:987–991. [PubMed: 10790869]
24. Valla J, Schneider L, Reiman EM. Age- and transgene-related changes in regional cerebral metabolism in PSAPP mice. Brain Res. 2006; 1116:194–200. [PubMed: 16942758]
25. Nicholson RM, Kusne Y, Nowak LA, LaFerla FM, Reiman EM, Valla J. Regional cerebral glucose uptake in the 3×Tg model of Alzheimer's disease highlights common regional vulnerability across AD mouse models. Brain Res. 2010; 1347:179–185. [PubMed: 20677372]

26. Valla J, Gonzalez-Lima F, Reiman EM. FDG autoradiography reveals developmental and pathological effects of mutant amyloid in PDAPP transgenic mice. Int J Dev Neurosci. 2008; 26:253–258. [PubMed: 18358666]
27. Reiman EM, Caselli RJ, Yun LS, Chen K, Bandy D, Minoshima S, Thibodeau SN, Osborne D. Preclinical evidence of Alzheimer's disease in persons homozygous for the e4 allele for apolipoprotein E. New Engl J Med. 1996; 334:752–758. [PubMed: 8592548]
28. Minoshima S, Foster NL, Kuhl DE. Posterior cingulated cortex in Alzheimer's disease. Lancet. 1994; 344:895. [PubMed: 7916431]
29. Reiman EM, Chen K, Alexander GE, Caselli RJ, Bandy D, Osborne D, Saunders AM, Hardy J. Functional brain abnormalities in young adults at genetic risk for late-onset Alzheimer's dementia. Proc Natl Acad Sci USA. 2004; 101:284–289. [PubMed: 14688411]
30. Valla J, Schneider LE, Niedzielko T, Coon KD, Caselli RJ, Sabbagh MN, Ahern GL, Baxter L, Alexander G, Walker DG, Reiman EM. Impaired platelet mitochondrial activity in Alzheimer's disease and mild cognitive impairment. Mitochondrion. 2006; 6:323–330. [PubMed: 17123871]
31. Valla J, Berndt JD, Gonzalez-Lima F. Energy hypometabolism in posterior cingulated cortex of Alzheimer's patients: Superficial laminar cytochrome oxidase associated with disease duration. J Neurosci. 2001; 21:4923–4930. [PubMed: 11425920]
32. Valla J, Yaari R, Wolf AB, Kusne Y, Beach TG, Roher AE, Corneveaux JJ, Huentelman MJ, Caselli RJ, Reiman EM. Reduced posterior cingulated mitochondrial activity in expired young adult carriers of the APOE e4 allele, the major late-onset Alzheimer's susceptibility gene. J Alzheimers Dis. 2010; 22:307–313. [PubMed: 20847408]
33. Frick KM, Baxter MG, Markowska AL, Olton DS, Price DL. Age-related spatial reference and working memory deficits assessed in the water maze. Neurobiol Aging. 1995; 16:149–160. [PubMed: 7777133]
34. Bimonte-Nelson HA, Francis KR, Umphlet CD, Granholm AC. Progesterone reverses the spatial memory enhancements initiated by tonic and cyclic oestrogen therapy in middle-aged ovariectomized female rats. Eur J Neurosci. 2006; 24:229–242. [PubMed: 16882019]
35. Morris RG, Garrud P, Rawlins JN, O'Keefe J. Place navigation impaired in rats with hippocampal lesions. Nature. 1982; 297:681–683. [PubMed: 7088155]
36. Valla J, Schneider L, Small A, Gonzalez-Lima F. Quantitative cytochrome oxidase histochemistry: Applications in human Alzheimer's disease and animal models. J Histotechnol. 2007; 30:235–247.
37. Paxinos, G.; Franklin, KBJ. The mouse brain in stereotaxic coordinates. San Diego: Academic Press; 2001.
38. Colton CA, Mott RT, Sharpe H, Xu Q, Van Nostrand WE, Vitek MP. Expression profiles for macrophage alternative activation genes in AD and in mouse models of AD. J Neuroinflammation. 2006; 3:27. [PubMed: 17005052]
39. Billings LM, Oddo S, Green KN, McGaugh JL, LaFerla FM. Intraneuronal Aβ causes the onset of early Alzheimer's disease-related cognitive deficits in transgenic mice. Neuron. 2005; 45:675–688. [PubMed: 15748844]
40. Hirata-Fukae C, Li H, Hoe H, Gray AJ, Minami SS, Hamada K, Niikura T, Hua F, Tsukagoshi-Nagai H, Horikoshi-Sakuraba Y, Mughal M, Rebeck GW, LaFerla FM, Mattson MP, Iwata N, Saido TC, Klein WL, Duff KE, Aisen PS, Matsuoka Y. Females exhibit more extensive amyloid, but not tau, pathology in an Alzheimer transgenic model. Brain Res. 2008; 1216:92–103. [PubMed: 18486110]
41. Lagouge M, Argmann C, Gerhart-Hines Z, Meziane H, Lerin C, Daussin F, Messadeq N, Milne J, Lambert P, Elliott P, Geny B, Laakso M, Puigserver P, Auwerx J. Resver-atrol improves mitochondrial function and protects against metabolic disease by activiating SIRT1 and PGC-1α. Cell. 2006; 127:1109–1122. [PubMed: 17112576]
42. Schmidt-Wilcke T, Poljansky S, Hierlmeier S, Hausner J, Ibach B. Memory performance correlates with gray matter density in the ento-/perirhinal cortex and posterior hippocampus in patients with mild cognitive impairment and healthy controls: A voxel based morphometry study. NeuroImage. 2009; 47:1914–1920. [PubMed: 19442751]
43. Braden BB, Talboom JS, Crain ID, Simard AR, Lukas RJ, Prokai L, Scheldrup MR, Bowman BL, Bimonte-Nelson HA. Medroxyprogesterone acetate impairs memory and alters the GABAergic

system in aged surgically menopausal rats. Neurobiol Learn Mem. 2010; 93:444–453. [PubMed: 20074654]

44. Carroll JC, Rosario ER, Chang L, Stanczyk FZ, Oddo S, LaFerla FM, Pike CJ. Progesterone and estrogen regulate Alzheimer-like neuropathology in female 3×Tg-AD mice. J Neurosci. 2007; 27:13357–13365. [PubMed: 18045930]
45. Carroll JC, Rosario ER, Kreimer S, Villamagna A, Gentzschein E, Stanczyk FZ, Pike CJ. Sex differences in β-amyloid accumulation in 3×Tg-AD mice: Role of neonatal sex steroid hormone exposure. Brain Res. 2010; 1366:233–245. [PubMed: 20934413]
46. Lee DC, Rizer J, Selenica ML, Reid P, Kraft C, Johnson A, Blair L, Gordon MN, Dickey CA, Morgan D. LPS-induced inflammation exacerbates phospho-tau pathology in rTg4510 mice. J Neuroinflammation. 2010; 7:56. [PubMed: 20846376]

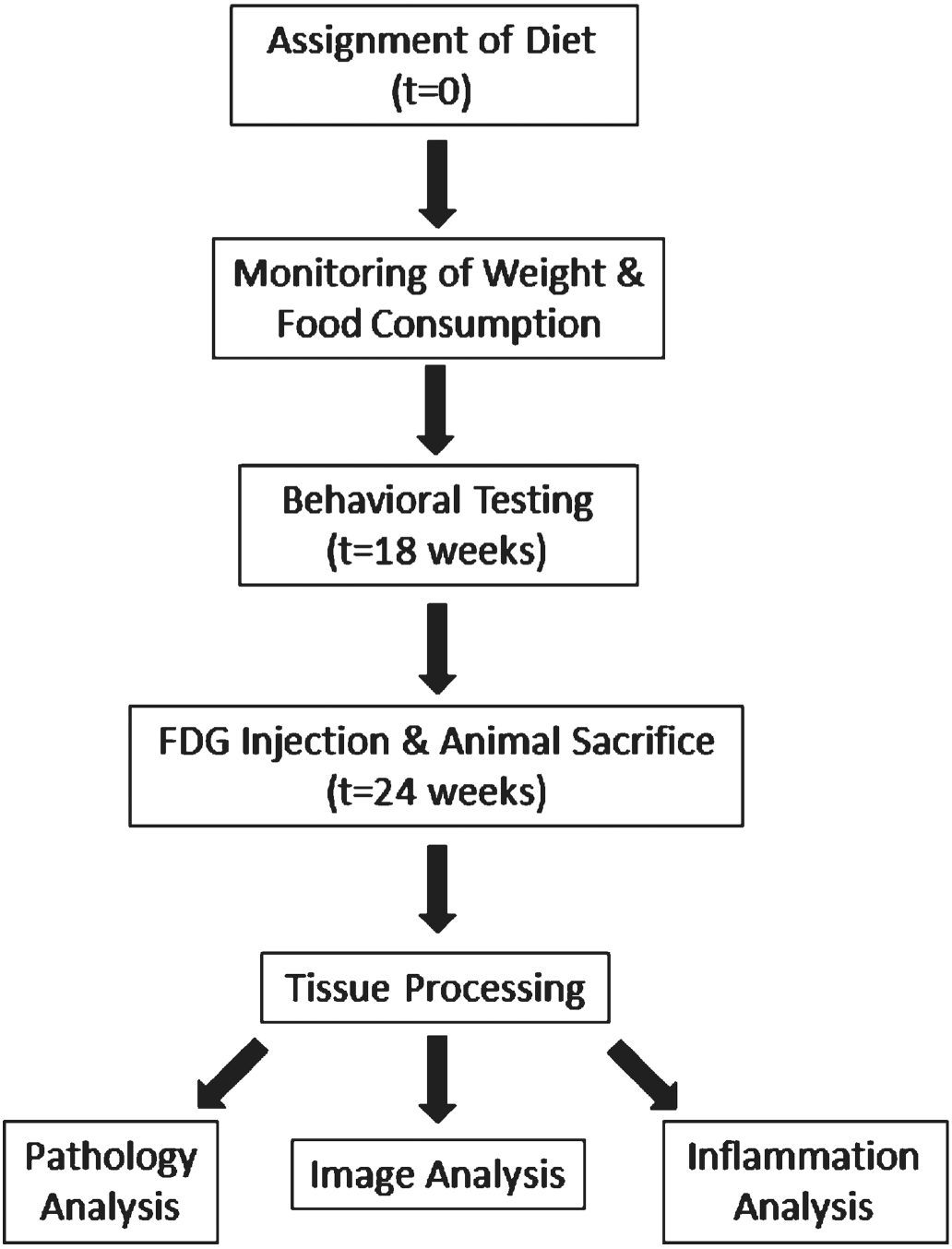

Fig. 1.
Flowchart summarizing each stage of the study. The same animals were used for each analysis throughout the study, with tissues distributed from the behaviorally-tested animals.

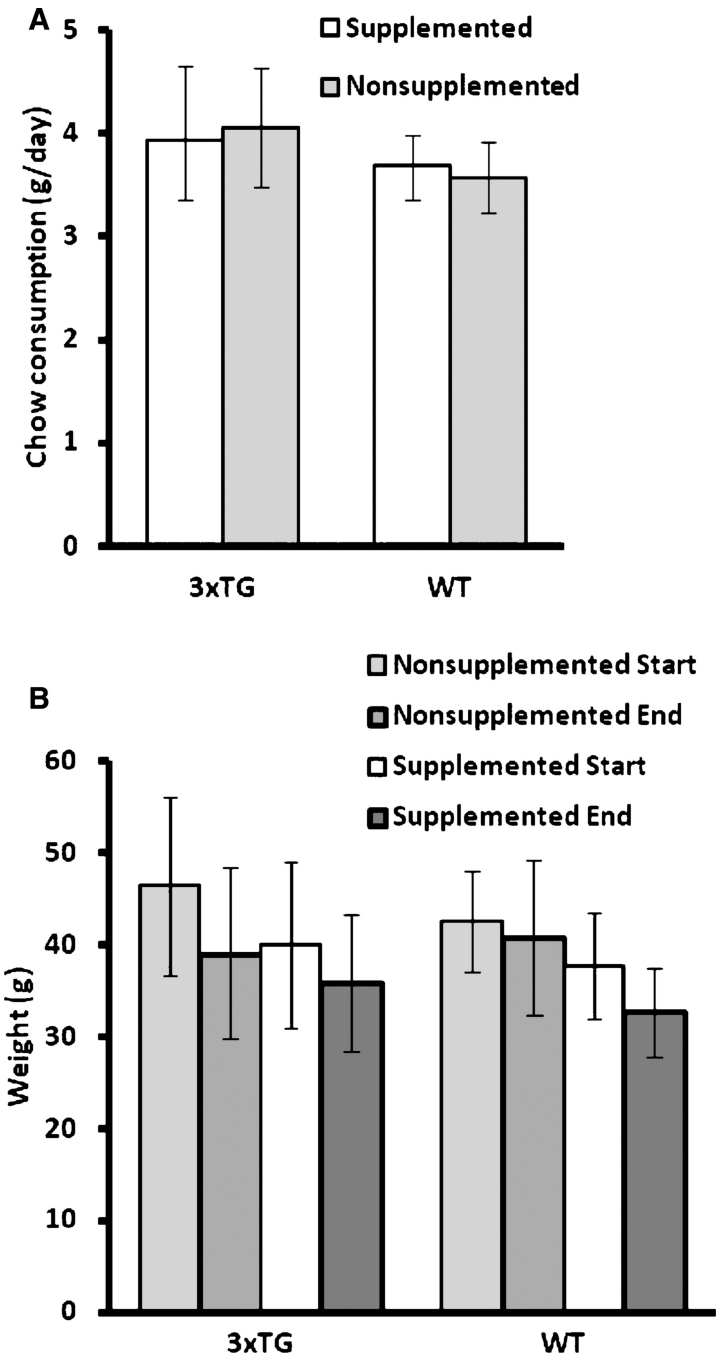

Fig. 2.

Mean (±standard deviation) chow consumed and body weight change during the protocol was not significantly different between 3×Tg and WT nor supplemented versus nonsupplemented. A) Mean chow consumption (g/day) for each group during the first three weeks of supplementation. B) Mean starting and ending body weights (g) for each group.

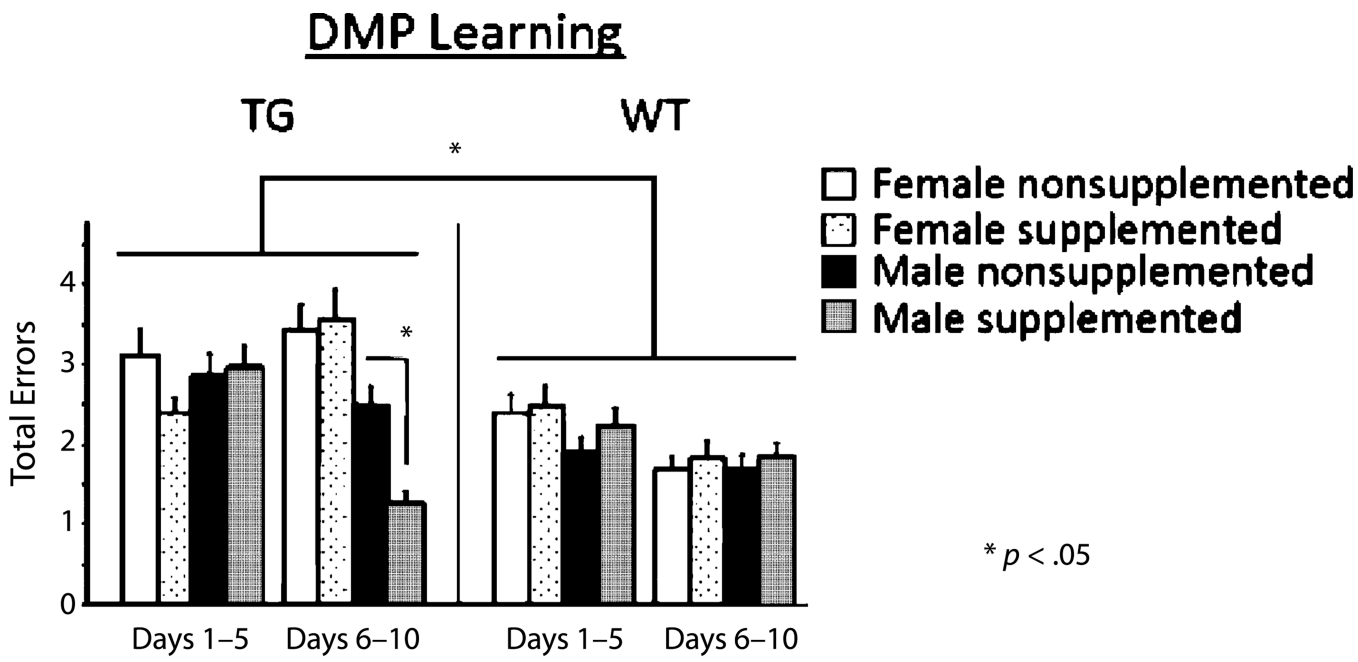

Fig. 3.
Mean error scores for total errors (±SE) on the delayed match to position for regular testing days 1–10, separated into learning (days 1–5) and asymptotic (days 6–10) phases.

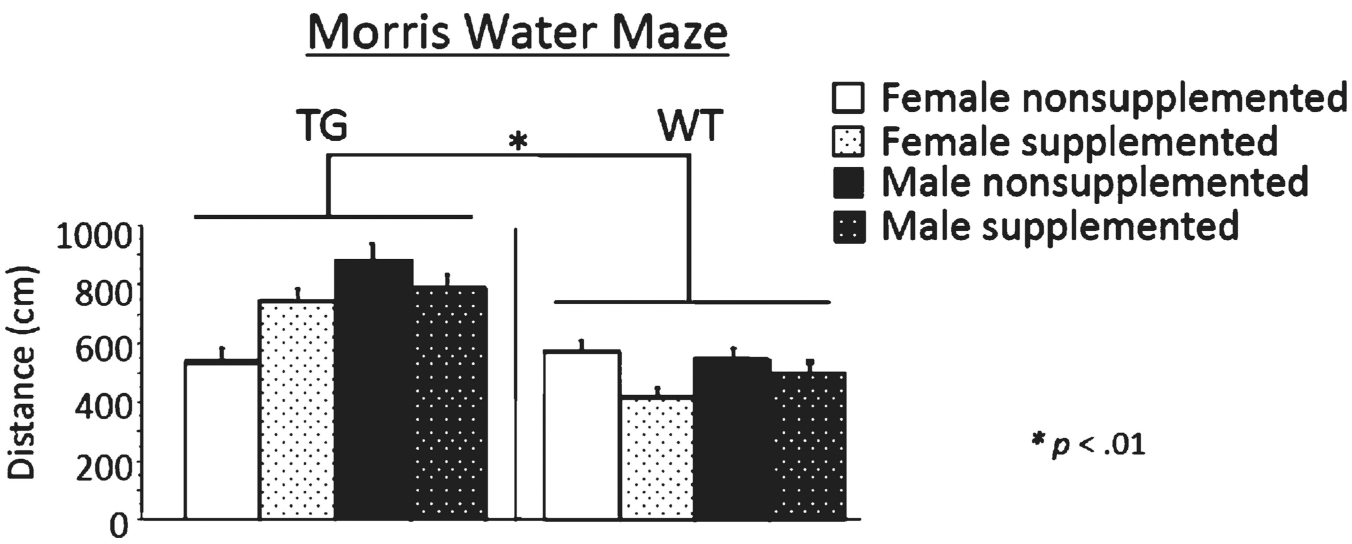

Fig. 4.
Mean distance scores in centimeters (±SE) on Morris maze days 1–6.

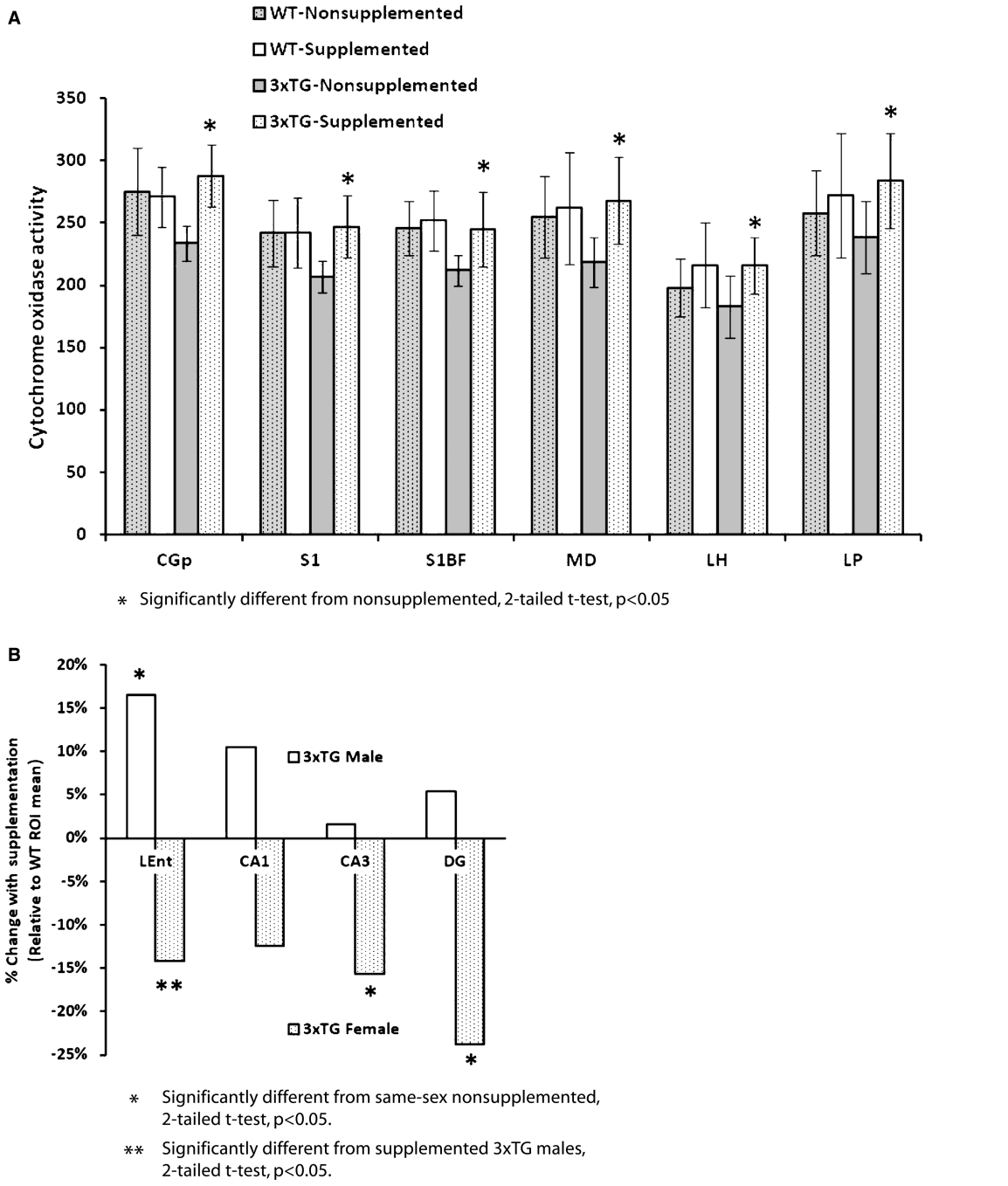

Fig. 5.

Mean (±standard deviation) cytochrome oxidase activity in select regions. A) ROIs demonstrating significant effects of supplementation, where supplementation significantly prevented or restored the region-specific cytochrome oxidase activity decline in 3×Tg mice. B) 3×Tg hippocampal ROIs demonstrated supplementation-driven differential sex effects, wherein the female 3×Tg mice decreased further from the WT means and the 3×Tg males improved toward the WT mean. Abbreviations as in Table 2.

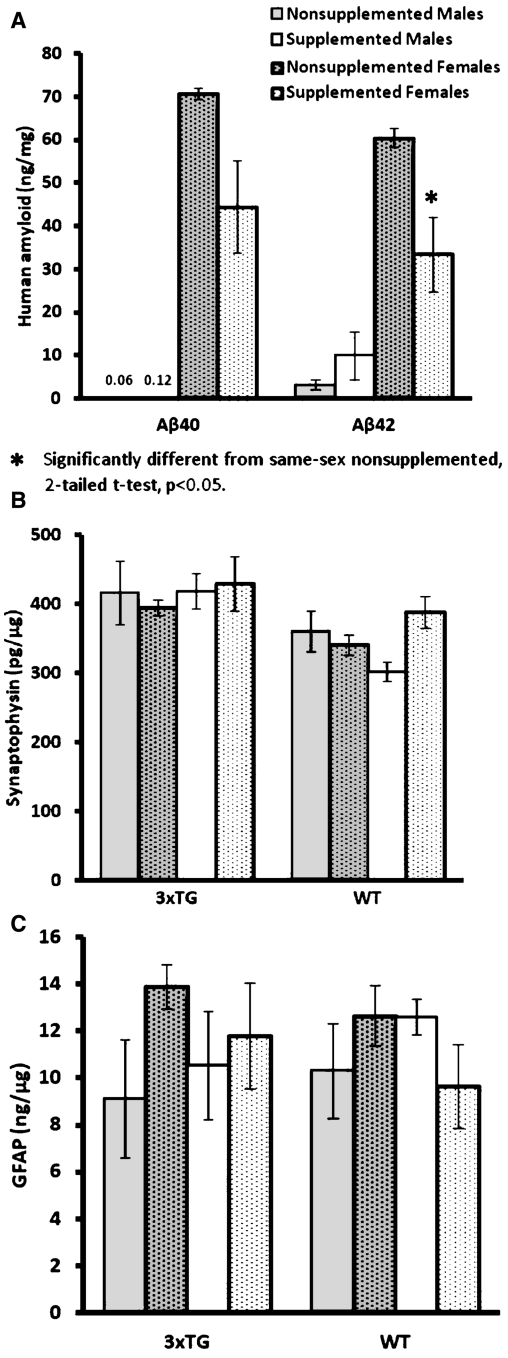

Fig. 6.

Mean (±SE) ELISA results. A) Female 3×Tg mice demonstrated significantly higher human Aβ levels than males. Supplementation only significantly reduced $A\beta_{42}$ levels in female 3×Tg mice, with $A\beta_{40}$ trending similarly. WT mice were not analyzed for human Aβ. B) Synaptophysin ELISA demonstrated no significant differences. C) GFAP (glial fibrillary acidic protein) ELISA demonstrated no significant differences.

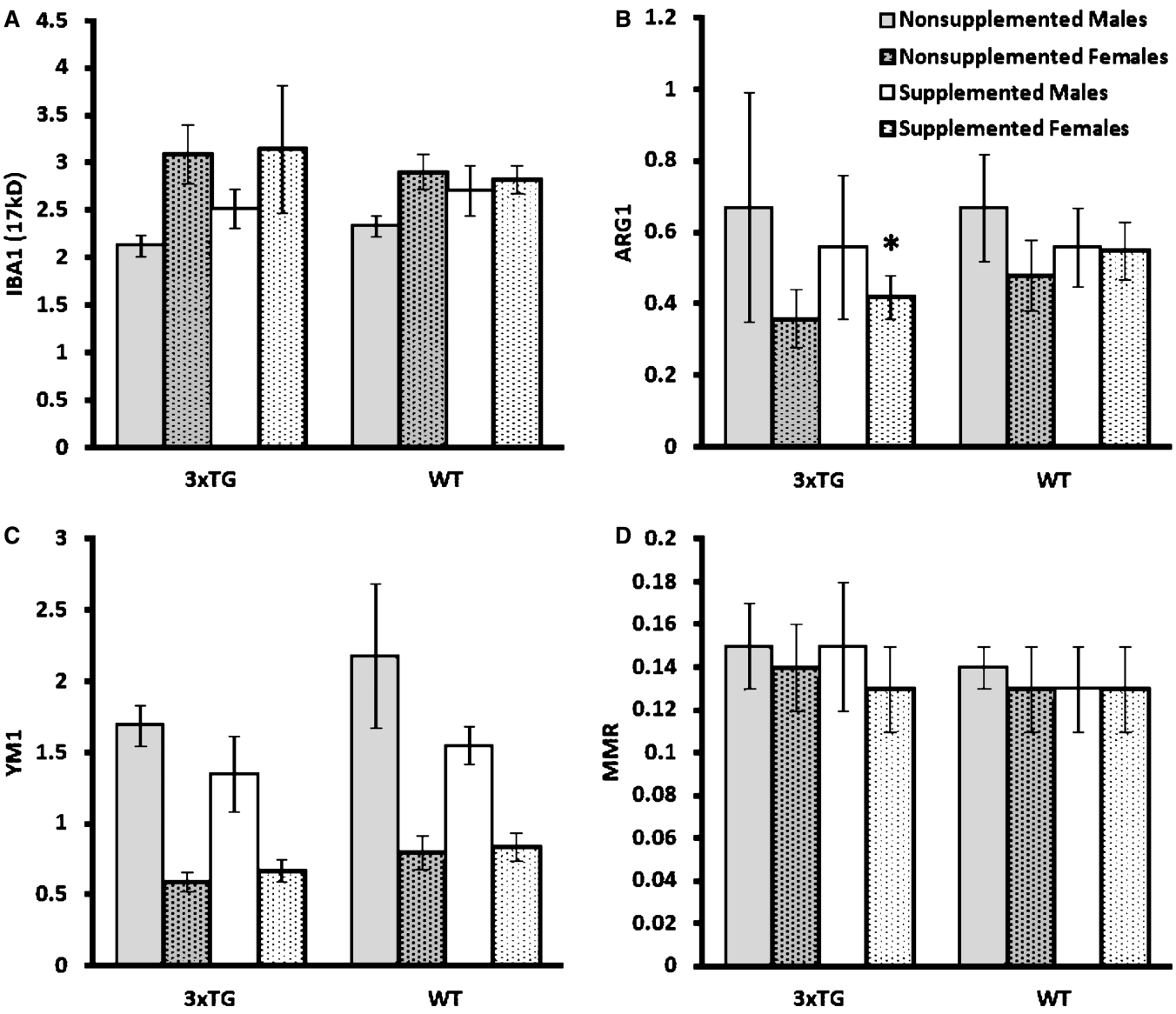

Fig. 7.

Mean (±SE) Western blotting results, normalized to β-actin. A) IBA1 (ionized calcium binding adaptor molecule 1) demonstrated no significant differences. B) ARG1 (arginase 1) demonstrated a significant increase in female 3×Tg mice after supplementation (2-tailed *t*-test, $p<0.05$). C) YM1 (chitinase 3-like 3) demonstrated no significant differences. D) MMR (macrophage mannose receptor) demonstrated no significant differences. *Significantly different from nonsupplemented 3×Tg females, 2-tailed *t*-test, $p < 0.05$.

Table 1

Summary of the 3 MPNSP supplements integrated into the mouse chow. Each was purchased over-the-counter at a local grocery

Freeze-dried phyto-nutrient powder (target: 5.25 mg/day/mouse)		
Blueberry	Cranberry	Parsley
Brown rice *	Ginger *	Pomegranate *
Brussels sprout *	Green cabbage *	Red cabbage *
Chicory *	Kale	Rose hip *
Cinnamon *	Okra *	Spinach
Concord grape *	Papaya *	Turmeric *
Herbal/spice liquid amalgam (target: 1.94 μl/day/mouse)		
Rosemary (leaf): supercritical & ethanolic extracts (23% total phenolic antioxidants)		
Turmeric (rhizome): supercritical (45% turmerones) & ethanolic extracts (7% curcuminoids)		
Ginger (rhizome): supercritical (30% pungent compounds) & ethanolic extracts (3% pungent compounds)		
Holy Basil (leaf): ethanolic extract (2% ursolic acid)		
Green Tea (leaf): hydroethanolic extract (45% polyphenols)		
Hu Zhang (root and rhizome): hydroethanolic extract (8% resveratrols)		
Chinese Goldthread (root): hydroethanolic extract (6% berberine)		
Barberry (root): hydroethanolic extract (6% berberine)		
Oregano (leaf): supercritical extract (4% total phenolic antioxidants)		
Baikal skullcap (root): hydroethanolic extract (17–26% baicalein complex, 0.4–0.9% wogonin)		
Other: extra virgin olive oil, maltodextrin, silica, yellow beeswax, palm kernel oil		
Cod liver oil (target: 6.56 μl/day/mouse)		
DHA	EPA	Vitamin D
20.40	16.10	15.00 mg/kg/day

* Cultured with following probiotic species, 1 billion per serving at the time of manufacture:

L. casei, L. plantarum, L. salivarius, L. acidophilus, L. rhamnosus, S. thermophilus, B. bifidum, B. infantis, B. longum, & B. breve

J Alzheimers Dis. Author manuscript; available in PMC 2013 September 16.

Table 2

Comprehensive list of all regions-of-interest assessed and the calculated probability values for each main effect and interaction from the 2×2×2 ANOVA on the cytochrome oxidase imaging data. Regions showing significant (*$p < 0.05$) main effects and interactions were assessed with post hoc 2-tailed *t*-tests

ROI	Genotype (G)	Diet (D)	Sex (S)	G×D	S×G	S×D	S×G×D
Optic tract (opt)	0.751	0.280	0.172	0.916	0.105	0.649	0.611
Cingulate gyrus, retrosplenial (RSG)	0.028*	0.539	0.376	0.648	0.909	0.350	0.058
Cingulate gyrus, posterior 2 (CGp2)	0.418	0.661	0.086	0.690	0.269	0.505	0.655
Cingulate gyrus, posterior (CGp)	0.105	0.001*	0.380	0.006*	0.298	0.829	0.635
Cingulate gyrus, middle (CGm)	0.063	0.225	0.211	0.606	0.571	0.433	0.947
Cingulate gyrus, anterior (CGa)	0.102	0.375	0.074	0.321	0.772	0.654	0.927
Posterior parietal cortex (PPtA)	0.139	0.951	0.058	0.754	0.562	0.691	0.554
Lateral entorhinal cortex (LEnt)	0.026*	0.316	0.560	0.394	0.689	0.008*	0.620
Primary somatosensory cortex (S1)	0.062	0.022*	0.389	0.018*	0.443	0.789	0.785
Primary somatosensory, BF (S1BF)	0.046*	0.066	0.225	0.289	0.909	0.857	0.512
Secondary somatosensory cortex (S2)	0.090	0.064	0.149	0.173	0.780	0.767	0.913
Primary auditory cortex (Au1)	0.020*	0.522	0.100	0.821	0.453	0.508	0.916
Primary visual, monocular (V1)	0.002*	0.737	0.302	0.986	0.299	0.989	0.025*
Piriform cortex (Pir)	0.841	0.862	0.350	0.764	0.648	0.805	0.171
CA1 (CA1)	0.002*	0.542	0.571	0.742	0.321	0.617	0.009*
CA3 (CA3)	0.005*	0.119	0.327	0.676	0.003*	0.989	0.018*
Dentate gyrus (DG)	0.170	0.348	0.526	0.125	0.743	0.242	0.008*
Subiculum (S)	0.001*	0.606	0.061	0.451	0.673	0.491	0.279
Medial mammillary nucleus (M)	0.869	0.359	0.563	0.505	0.251	0.275	0.008*
Substantia nigra (SNR)	0.131	0.964	0.273	0.600	0.457	0.019*	0.730
Basolateral amygdala (BLA)	0.372	0.056	0.262	0.168	0.924	0.938	0.882
Anteroventral thalamus (AV)	0.958	0.828	0.779	0.517	0.485	0.398	0.623
Reticular thalamus (Rt)	<0.001*	0.149	0.367	0.402	0.471	0.553	0.013*
Reuniens nucleus (Re)	0.639	0.461	0.278	0.778	0.479	0.897	0.436
Ventromedial thalamus (VM)	0.296	0.127	0.137	0.188	0.965	0.688	0.693
Ventrolateral thalamus (VL)	0.023*	0.021*	0.090	0.175	0.965	0.570	0.600
Mediodorsal thalamus (MD)	0.116	0.009*	0.438	0.053	0.362	0.148	0.585
Laterodorsal thalamus (LD)	0.051	0.391	0.267	0.614	0.311	0.150	0.073

ROI	Genotype (G)	Diet (D)	Sex (S)	G×D	S×G	S×D	S×G×D
Lateral posterior thalamus (LP)	0.599	0.010*	0.620	0.183	0.375	0.088	0.593
Parafascicular thalamus (PF)	0.112	0.792	0.062	0.823	0.462	0.695	0.268
Ventroposterolateral thalamus (VPL)	0.230	0.183	0.609	0.400	0.710	0.919	0.153
Ventroposteromedial thalamus (VPM)	0.168	0.677	0.057	0.629	0.368	0.763	0.346
Posterior thalamus (Po)	0.155	0.310	0.227	0.539	0.777	0.731	0.372
Lateral habenula (LHb)	0.806	0.683	0.450	0.380	0.935	0.454	0.448
Rostral caudoputamen (rCPu)	0.181	0.018*	0.269	0.837	0.539	0.755	0.735
Caudal caudoputamen (cCPu)	0.021*	0.790	0.224	0.360	0.643	0.991	0.242
Lateral globus pallidus (LGP)	0.228	0.706	0.301	0.928	0.797	0.963	0.999
Subthalamus (STh)	0.269	0.366	0.099	0.689	0.276	0.909	0.727
Nucleus accumbens (Acb)	0.742	0.216	0.318	0.869	0.384	0.668	0.592
Nuc. of vertical diagonal band (VDB)	0.409	0.205	0.303	0.277	0.875	0.514	0.749
Medial septal nucleus (MS)	0.936	0.246	0.170	0.376	0.803	0.840	0.947
Lateral septal nucleus (LSI)	0.100	0.096	0.183	0.893	0.872	0.990	0.883
Nucleus basalis (B)	0.043*	0.099	0.333	0.389	0.325	0.235	0.162
Anterior hypothalamus (AH)	0.337	0.634	0.063	0.708	0.150	0.602	0.935
Lateral hypothalamus (LH)	0.387	0.004*	0.478	0.436	0.935	0.737	0.699
Dorsolateral geniculate (DLG)	0.196	0.291	0.102	0.839	0.443	0.366	0.360
Medial geniculate (MG)	<0.001*	0.354	0.008*	0.080	0.236	0.022*	0.499
Superior colliculus (SC)	0.001*	0.281	0.052	0.120	0.516	0.055	0.968
Pontine nuclei (PnC)	0.111	0.394	0.598	0.362	0.744	0.826	0.132
Inferior colliculus, central (CIC)	0.267	0.051	0.500	0.420	0.278	0.365	0.003*
Periaqueductal gray (PAG)	0.114	0.226	0.975	0.938	0.523	0.405	0.091
Vestibular nuclei (Ve)	0.956	0.048*	0.950	0.614	0.299	0.936	0.222
Reticular nucleus, giganto (Gi)	0.605	0.095	0.633	0.930	0.958	0.258	0.865
Cerebellar lobules 1–5 (Cb)	0.008*	0.763	0.133	0.858	0.870	0.244	0.592
Simple lobule (Sim)	0.081	0.936	0.042*	0.370	0.994	0.160	0.393
Crus 1 lobule (Crus1)	0.043*	0.349	0.191	0.256	0.884	0.100	0.958